Refereed Proceedings

The 12th International Conference on Fluidization - New Horizons in Fluidization Engineering

Engineering Conferences International *Year* 2007

Measuring the Gas-Solids Distribution in Fluidized Beds - A Review

J. Ruud van Ommen* Robert F. Mudde†

*Delft University of Technology, The Netherlands, j.r.vanommen@tudelft.nl

†Delft University of Technology, The Netherlands

MEASURING THE GAS-SOLIDS DISTRIBUTION IN FLUIDIZED BEDS – A REVIEW

J. Ruud van Ommen and Robert F. Mudde
Delft University of Technology – Faculty of Applied Sciences
Julianalaan 136, 2628 BL Delft, The Netherlands
T: +3115 278 2133; F: +3115 278 5006; E: j.r.vanommen@tudelft.nl

ABSTRACT

This paper reviews techniques for measuring the voidage distribution in gas-solid fluidized beds, with a focus on the developments during the last ten years. Most attention is given to recent progress in tomography and pressure measurements, but visual observations, capacitance probes and optical probes are also covered.

INTRODUCTION

Gas-solid fluidized beds are extensively studied in academia and widely applied in industry. In the vast majority of cases, the distribution of the particles varies both in time and space. Bubbling fluidized beds have a more or less continuous dense phase and dispersed voids or 'bubbles', turbulent fluidized beds are characterized by elongated and irregular voids along with violently moving particle strands, and in fast fluidization we typically see a dilute core and a dense, downward moving wall layer. The gas-solids distribution and its variation have a strong effect on the various processes taking place in the system. For example, the presence of bubbles severely influences mixing and possible segregation of particles in a fluidized bed. Moreover, the conversion of gaseous reactants in fluidized bed reactors strongly depends on the size of voids and their solids content. The core-annulus structure in risers has a large impact on the particle-to-wall heat transfer. Therefore, it is of great importance to have the possibility to accurately determine the gas-solids distribution. Two characteristics of dense gas-solids flow make this a challenging task: the voidage distribution is changing quickly over time (i.e., a high temporal resolution is needed) and dense gas-solids flows are (with few exceptions) opaque to visible light. The latter point makes laser-based and other optical techniques, which have been proven to be very useful in single-phase and dilute two-phase flow, only of limited use in dense gas-solids flow.

In the past, a number of excellent reviews have been published on measurement techniques for fluidized beds, for example by Grace and Baeyens (1), Cheremisinoff (2), and Yates and Simons (3). More recently, Louge (4) reviewed experimental techniques for circulating fluidized beds. Werther (5) gave an overview of measurement techniques in fluidized beds, with emphasis on applicability in industrial practice. Chaouki et al. (6) extensively reviewed non-invasive measurement techniques for multiphase flows in general. This paper describes the principal experimental techniques to determine the voidage distribution in dense gas-solid fluidized beds; we will mainly focus on the developments over the last ten years.

DIRECT VISUALISATION

Visual observation is, in principle, a straightforward manner to obtain information about the voidage distribution. However, because of the opaque nature of a gas-solid fluidized bed its use is limited to the very dilute systems, the outer layer of a fluidized bed, and pseudo 2-D beds. To facilitate visual observation through transparent walls of materials such as glass or perspex, it is important to prevent excessive sticking of particles to the wall due to electrostatics. Possible measures are adding moderate quantities of fine salts to the bed, coating the walls with a conductive wax, or humidifying the fluidizing gas (4). Video recordings make it possible to observe in slow-motion phenomena that are too fast for the eye. For example, Horio and Hiroaki (7) used video recording to study cluster behaviour in a circulating fluidized bed and a bubbling bed freeboard. They obtained a clear image by applying a laser sheet perpendicular to the viewing direction. Image processing can be used to improve the quality of obtained recording (e.g., 8). In addition, it can be used to extract quantitative information, for example about the bubble size and velocity (9,10) or the segregation of particles (11) in pseudo 2-D beds. While the translation of results obtained in pseudo 2-D beds to 3-D systems must be done with caution, the use of pseudo 2-D beds can be valuable for, e.g., calibration of other types of measurement equipment and for validation of simulation codes.
An alternative to using visual imaging is X-ray imaging: an X-ray source is placed on one side of the bed, while a camera is placed at the other side of the bed (12). In this way, Yates et al. (13) determined in detail the voidage distribution around a bubble. However, this technique is less suited to visualize multiple bubbles, since it just shows a 2D projection of the 3D objects. This can be solved with tomographic techniques, which will be treated in the next section.

TOMOGRAPHY

Tomography literally means ‘writing a slice’. It is a non-intrusive technique that can be used for the reconstruction of the cross-sectional distribution of the different phases in a multiphase flow system such as fluidized beds. It relies on the measurement of a physical quantity that is different between the existing phases, gas and particles in our case. There are a wide variety of tomographic techniques, which can be divided into two groups:
1. Hard-field tomography. In this type of tomography, a uniform narrow field is set-up, which depends only on the local gas-solids distribution inside the measured cross-section; a particular field line is not influenced by the distribution outside this field line. In other words, the field lines are straight; this type is sometimes also referred to as linear-line or linear-field tomography. In fluidization research, mainly X-ray and gamma-ray tomography are used. Below, these types will be discussed more in depth.
2. Soft-field tomography. In this case, the gas-solids distribution influences the field lines. Typically, this results in non-linear field lines which makes reconstruction much more troublesome. Most soft-field tomographic techniques are based on the interaction of an electric field with the studied system (14). *Electric impedance tomography* (or electric resistance tomography) can be applied to flows having an electrically conductive continuous phase; it is therefore less suited for investigating

gas-solids flows. *Electromagnetic tomography* measures the permeability distribution of ferro-magnetic materials. *Displacement current tomography* is based on the current induced by moving charged particles (15). This technique is not only sensitive to the particle charge but also to the particle velocity. The only type of electric tomography that is widely applied in fluidization research is *electric capacitance tomography* (ECT). It will be discussed more in detail below.

Electric capacitance tomography

Most particles used in fluidized beds consist of a dielectric material (i.e., they are insulators), which means that they tend to concentrate an electric field within themselves. ECT makes use of the difference in dielectric constant between the particles and the fluidizing gas, which is typically large. For ECT, a number of plate electrodes (e.g., 16) are placed at a given height around the column. The electrodes are excited (or "fired") one by one and the capacitance values between the excited electrode and the remaining ones are measured, yielding $N(N-1)/2$ independent measurements for N electrodes. This is because capacitance $C_{i,j}=C_{j,i}$ and $C_{i,i}$, i.e. the self-capacitance, is not measured. The measurement protocol as described can be imagined as a rotation of the electrical field around the pipe cross-section in discrete steps with an angle $\alpha=360°/N$ (16). This is analogous to the source-detector movement in computerised tomography used in medical imaging. In most ECT systems, the frequency of the electrical signal that imposes the electrical field in the measurement domain is of the order of 1MHz. This allows the measurement time per electrode-pair to be kept short. This is an advantage over the nuclear techniques, where speed is an issue. ECT-data can be captured fast enough to allow measuring up to 1000 frames/sec (17,18).

The governing equation relating the permittivity distribution, $\varepsilon(x,y)$ (which is directly connected to the solids distribution) to the electric field potential, $\phi(x,y)$, is $\nabla\cdot\left[\varepsilon(x,y)\nabla\phi(x,y)\right]=0$. The measured capacitances, $C_{ij}=\dfrac{Q_i}{\Delta V_{ij}}$, with ΔV_{ij} the voltage difference between electrode i and j and $Q_i=\oint\varepsilon(x,y)\nabla\phi(x,y)\cdot\hat{n}dl$, the induced charge on sensor i, link the measured data to the permittivity distribution. The task of the reconstruction is to translate the obtained capacitance data back into a dielectric distribution (which can be interpreted as a phase distribution for two-phase flows over the cross-section). However, this translation or reconstruction is troublesome, since the unknown solids distribution influences the electric field. The problem to solve is highly non-linear and shows the soft-field characteristics.

The commonly used algorithm to reconstruct the voidage distribution is the linear back projection (LBP) algorithm. The algorithm is based on the sensitivity matrix, $\boldsymbol{S}$, which is the response of a particular electrode-pair to a small change of the otherwise uniform permittivity distribution in a particular location. In mathematical terms: $C = \boldsymbol{S}\cdot G$, with G the image vector. LBP solves this (usually ill-posed) problem by approaching $\boldsymbol{S}^{T}\cdot\boldsymbol{S}$ by the identity matrix. It is fast, but of relatively low quality. Various methods have been developed to improve the image quality; see Liu et al. (19) for a recent overview. Generally speaking, these can be classified in two categories: iterative algebraic reconstruction techniques (the ART-family, see below) and neural networks. These methods clearly outperform LBP, but at a much higher computational cost. For real time applications, LBP is at present the only alternative. However, obtaining good spatial resolution remains a major challenge in ECT. In addition, the presence of electrostatic charges in the imaging domain negatively influences the validity of ECT maps (20). Another challenge is reconstructing solids distribution maps for systems of which the particle permittivity changes over time, e.g., due to drying. Chaplin et al. (21) developed a calibration scheme to account for this and validated it with X-ray tomography.

A recent development is the reconstruction of 3D images of the solids distribution using ECT. Liu et al. (19,22) describe a technique to generate quasi-3D images by making a smooth interpolation between subsequent 2D maps. Fan et al. (20) proposed electrical capacitance volume tomography (ECVT) to obtain truly instantaneous 3D images. In conventional 2D ECT, the image obtained is the projection of the solids distribution on a cross-section by assuming no axial variation. This is a disputable assumption, since ECT electrodes are typically some centimeters high. Moreover, due to the soft field, the field lines are not necessarily confined to the slice defined by the electrodes. In ECVT, the real-time 3D whole-volume solids distribution is reconstructed in the region enclosed by the geometrically 3-D capacitance sensor. In Warsito et al. (23), 3D reconstructions are presented from simulated data as well as from real applications, namely a gas-liquid flow. The reconstruction technique is based on neural networks.

X-ray and gamma-ray tomography

A second class of tomographic techniques makes use of ‘nuclear’ fields. Here, a source generates high-energy photons that travel through the fluidized bed. The measurement principle is transmission. For a monochromatic beam of high energy photons with initial intensity I_0, the Lambert-Beer law describes the transmission through a material of constant density; $\frac{I(x)}{I_0}=\exp(-\mu x)$ with μ the attenuation coefficient, x the thickness and $I(x)$ the intensity after passage. For a beam along a path of varying density, i.e. varying attenuation, the measured intensity is the integral effect of the local attenuation with the local attenuation coefficient: $\frac{I(x)}{I_0}=\exp\left[-\int \mu(x)dx\right]$. Due to the high energy, the photons travel in straight lines. Only via an interaction with the fluidizing material will they deviate from this line upon which they are not measured. By measuring over a large number of independent lines, sufficient information can be collected for a tomographic reconstruction.

Compared to Electrical Tomography, the nuclear techniques are slow. This is a consequence of safety issues and the random nature with which the photons are generated when employing nuclear sources such as ^{137}Cs. The latter creates inherent noise in the measured beam intensity, which drops off as the inverse of the square root of the number of photons counted. Consequently, the measuring time cannot be made short without the use of excessively strong sources. On the other hand, a high number of beams can easily be used. Thus, the number of independent measurements per tomogram can be made large. This is what is done in medical applications, where the source-detector system is rotated around the object of interest. Therefore, high spatial resolution images can be obtained. However, rotating the measuring system is also a slow process. Therefore, usually the frame rate is on the order of 1 frame/sec, clearly insufficient for any dynamic study in fluidization. Time averaged information can be obtained with good accuracy (see e.g., 24,25). Mudde et al. (25) used two sources-detectors separated by a small vertical distance to study some dynamical aspects of their fluidized system. As an alternative, rather than rotating the source-detector, several sources could be used simultaneously. Bruneau et al. (26,27,28) investigated numerically the possibility of a

3 and 5 sources scanner with measuring times per tomogram ranging from several seconds to 1ms (see Fig. 1). They mimicked a 100mCi ^{137}Cs source measuring through a 40cm diameter fluidized bed and concluded that good accuracy could be obtained using the 5-source system, i.e. a measuring time of 10ms would still provide a spatial resolution of 10mm.

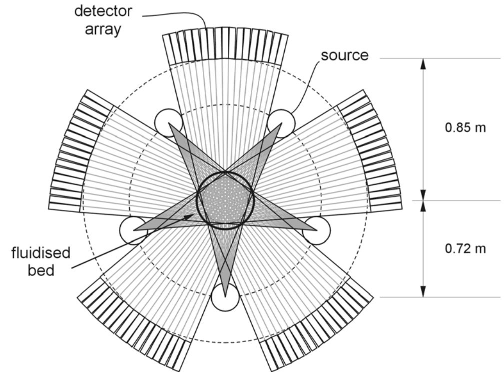

Fig. 1 The five -source system studied by Bruneau et al. (26,27).

The measured beam attenuation can directly be turned into the mean chordal void fraction, $\overline{\alpha}$, called the ray sum, p_i. As the attenuation is a local phenomenon, the ray sum is the integral effect along the beam path. This can easily be discretized using pixels, resulting in the system $p_i = W_{ik}\alpha_k$ with α_k the averaged void fraction of pixel k and W_{ik} the length of the beam i through pixel k (see Fig. 2). This problem is similar to the LBP one and can be solved with similar techniques. However, here the problem is not linearized from an intrinsic non-linear one.

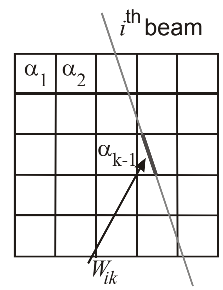

Fig. 2 Pixel based reconstruction.

Due to measurement noise, the actual problem is formulated as $\vec{p} = \mathbf{W}\cdot\vec{\alpha} + \vec{\varepsilon}$ where ε takes the noise into account. The Algebraic reconstruction methods (the ART family) solves this problem by minimizing the mismatch between $\vec{p}$ and $\mathbf{W}\cdot\vec{\alpha}$. For instance, the ART uses the algorithm

$$\alpha_k^{n+1} = \alpha_k^n + \sum_i \frac{p_i - \sum_j W_{ij}\alpha_j}{\sum_m W_{im}^2} W_{ik}$$

Various adaptations of this algorithm exist and several forms of regularizations are around that improve the capabilities of the reconstruction. Figure 3 shows the reconstruction of three circular objects from synthetic data. The system mimicked is a fluidized bed of 23cm. The gap between the two large objects is less than 1cm. The reconstruction algorithm has no trouble keeping the two objects separated. The small object has a diameter of 2cm and is also reconstructed reasonably well.

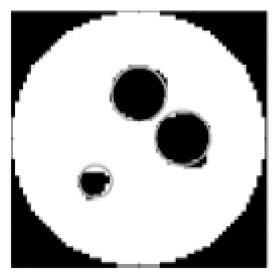

Fig. 3 Reconstruction of three 'bubbles' using an adapted ART algorithm.

In medical applications, X-ray tubes are used to generate the photons. This has the advantage that high intensities can be easily reached. Moreover, the photon energy is relatively low compared to many nuclear sources. This makes safety less complicated and expensive. However, an X-ray source generates a wide spectrum of photon energies. As a consequence, the absorption is no longer governed by a single attenuation coefficient and beam hardening occurs: the low energy photons are attenuated more effectively. This is in principle a function of the unknown void fraction and poses a potential problem. However, the use of an effective attenuation coefficient is a practical way of circumventing this problem.

In a recent paper, Tortora et al. (29) compared a 16 electrode ECT system with a gamma-densitometer (GDT) based on a 100mCi ^{137}Cs source with 8 detectors. They studied the solids distribution in a gas-solid riser of 14cm diameter circulating fluidized bed. With the GDT, only accurate solids distributions in a time averaged sense could be obtained. Moreover, the solids distribution was reconstructed using the Abel transform on a single view through the riser. A quantitative comparison between the ECT and GDT was also made. From the data it could be concluded, that the distributions obtained from ECT and GDT are in good agreement over a wide range from almost close packing at the wall (solids fraction ~0.66) to very dilute in the core. The typical differences between the solids volume fractions from the two techniques, is reported to be below 0.03. This work shows that both techniques can give identical and reliable results.

Simpler versions of tomography using nuclear sources are used more frequently. Only one source is used, either in combination with a single detector (single beam arrangement, 25,30,31) or a number of detectors (fan beam configuration, 29,32). The former requires a single traverse through the slice of interest, the latter provides these data in one capture. Due to the single view, insufficient information for true tomographic reconstruction is available. However, time-averaged reconstructions, assuming symmetry, are possible. In essence, the Abel transform (33) is used to turn the set of line-averaged data in the solids distribution into a cross-section. Care should be taken as error propagation can be severe (25). The vast majority of reports on this form of GDT concern bubbly flows; fewer reports are found for gas-solid systems.

OPTICAL PROBES

Optical probes for measuring the solids distribution have been around for a long time. They find applications in cold flow models but have also been used in fluidized beds operating at high temperatures (e.g., 34). Various configurations exist, but they can be coarsely classified as reflection or transmission probes. The reflection probes have the sending and receiving optics (usually a glass fiber) at the same side. Light is sent into the powder and the reflections are recorded. One of the problems is the lack of a properly defined measuring volume; in dilute systems the light can travel quite a distance from the probe before a reflecting particle is encountered. This can be overcome by a clever arrangement of the sending and receiving end. In Rundqvist et al. (35) such a design is discussed (see Fig. 4). The two fibers are placed at 45º. An extra glass window is mounted on their ends to create a measuring volume directly in front of the probe. This way a monotonic response to the local solids fraction is ensured. The probe used in the hot experiments of Johnsson and Johnsson (34) has in essence a similar design.

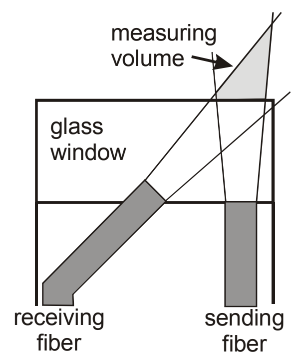

Fig.4 Optical probe of Rundqvist et al. (35).

Background light can easily be removed by using a pulsed light source. During the period the source is off, the background light is detected, which can then be subtracted from the reflection signal. With modern light sources, e.g. LEDs, a high pulsation frequency can easily be achieved, effectively removing background noise without compromising the sampling rate.

Liu et al. (36) used a reflection type probe to measure both the solids concentration close to the probe as well as the solids velocity, thus obtaining the local solids flux. They used a three-fiber arrangement, with the sending fiber in the center. By applying a glass window in front of the fiber ends, the possible interference of particles moving too close to the probe for accurate detection is eliminated. The signals from the two receiving fibers were cross-correlated to find the time of flight of particles from one receiver to the other. This provides a velocity estimate; many researchers have used this technique (see, e.g., 37). By choosing a large fiber diameter as compared to the particle diameter, the cluster of particles in front of the probe contribute to the reflected light giving a continuous signal. Via a suitable calibration procedure, this signal was converted into the local particle concentration.

A different approach to create a well-defined measuring volume is followed by Nova et al. (38). They used a so-called GRIN lens to focus the diverging beam from the sending fiber. The measuring volume is formed by the high light intensity of the waist of the converging beam after the lens. The authors discuss that particles closer to the lens do not contribute to the signal recorded. Consequently, the measuring volume is pushed away from the end of the probe, making it less prone to the probe distortion of the flow.

The second class of optical probes used for assessing the solids fraction are transmission probes. Here the sending and receiving fibers are facing each other. If 'no' solids are present in the gap between sender and receiver the light transmits freely and is detected. This probe is especially useful for detecting voids or bubbles (39,40). The probe of Groen et al. (40) consists of a double set sender-receiver. This allows estimates of the vertical component of the bubble velocity (time of flight) and of the bubble size distribution (velocity times duration of the bubble signal). For the latter, a bubble shape needs to be assumed, as it is impossible from the signals to say whether a small bubble is hit at the center or a small bubble at the side. Clark and Turton (41) describe a technique to turn the probability density function (pdf) of the measured pierced length of the bubbles into the pdf of the bubble diameter, for a given shape of the bubbles. The probe data has been validated against video images using a pseudo 2D fluidized bed.

CAPACITANCE PROBES

Whereas the electrodes used in ECT span the whole bed, a capacitance measurement with two closely spaced electrodes can be used to determine the voidage in a small measurement volume. Originally, two parallel flat plates were used. However, in an attempt to improve the design, Werther and Molerus (42) devised a needle probe: a protruding, downward pointing needle forms the sensor electrode, while the enclosing metal tube forms the ground electrode. The benefit of this miniaturized probe is that it causes very little disturbance of the flow. Several other researchers followed this approach and used a similar design. Almstedt and Olsson (43) added water-cooling to this probe type for use in hot units. Acree Riley and Louge (44) incorporated a third conductor, a 'guard electrode', in their flat plate capacitance probe. Later, Soong et al. (45) did the same for a needle probe. The guard electrode surrounds this sensor electrode and is kept at exactly the same voltage as the sensor. In this way, it absorbs most electric field disturbances for outside sources: cable capacitance and 'stray capacitance' due to nearby electrical surfaces are eliminated, which leads to a more accurate and reproducible signal (4). Louge et al. (46) described a non-invasive wall-probe: by incorporating a sensor, ground, and guard electrode in the wall, a small measurement volume is created, penetrating approximately 2mm into the bed. This type of probe is very convenient to study the wall clusters in circulating fluidized bed risers, since very small irregularities can already disturb the flow pattern in these systems (47). Louge (4) and Wiesendorf and Werther (48) give a more extensive overview of the developments on capacitance probes up to 1997 and 2000, respectively. After 2000, remarkably little has been published in fluidization literature about improvements of capacitance probes.

PRESSURE MEASUREMENTS

Time-averaged pressure measurements

Pressure measurements are cheap and relatively easy to perform, and therefore widely applied in fluidized beds. Time-averaged pressure measurements are used both in lab-scale setups and in commercial units. In fact, together with temperature measurements – which fall outside the scope of this review – it is the only measurement technique that is applied in industry on a routine basis (5). Measuring the pressure difference Δp between two positions with a vertical spacing h gives an estimate for the average bulk density between these positions: $\rho_{bulk} \approx \Delta p / [h \bullet g]$. In circulating fluidized beds, a number of pressure taps distributed over the height of the riser can be used to give an indication of the density as a function of height. However, deviations can be expected at positions with a strong change in voidage or particle velocity (4). In bubbling and turbulent fluidized beds, measuring the pressure difference between a point below and a point above the bed surface gives the possibility to estimate the bed height when the average bulk density of the bed is known.

Time-resolved pressure measurements

When the pressure is sampled at a sufficiently high frequency, the pressure fluctuation signal obtained can yield much more information about the fluidized bed hydrodynamics. These time-resolved or dynamic pressure measurements are widely applied in fluidized bed research, whereas application in industry is still scarce. The sample frequency used for pressure fluctuation measurements depends on the system under investigation and on the way the pressure signals will be analysed, but 20Hz can be considered as a lower limit. Typically, a sample frequency in the order of 200Hz is applied.

Pitfalls in measuring pressure fluctuations

Even when suitable sensors with a high enough response frequency are used, several pitfalls are encountered in practice. To obtain good measurements, the following points should be taken into account:

1. *Dimensioning of the probe-transducer system.* In most cases, the pressure transducer is not in direct contact with the bed, but connected to it with a probe or tube. In order to minimize resonance effects, it is recommended to keep the probe length as short as possible. The inner diameter of the probe is preferably between 2 and 5mm (49). Smaller diameters lead to dampening of the signal. Larger diameters increase resonance effects and increasingly disturb the local hydrodynamics, especially when a purge flow is applied.

2. *Free entrance of the probe.* One solution to avoid blocking of the probe entrance is to cover it with a wire mesh. As long as the mesh is open enough, it has no significant influence on the pressure fluctuations (49). An alternative is to apply a constant purge flow. This flow should be high enough to prevent particles from entering the probe, but low enough to avoid (excessive) bubble formation at the probe tip. Recommended values are 0.5-1.0m/s for Geldart A particles (50,51) and 1.0-.2.0m/s for Geldart B particles (52).

3. *Proper placement of the probe(s).* Pressure probes are often placed flush with the wall, as this minimizes the disturbances of the bed hydrodynamics. Croxford et al. (53) report that for a small-scale fluidized bed, in principle, one probe is sufficient to characterize the hydrodynamics. However, when the bubble size as a function of height should be obtained, several probes will be needed. Van Ommen et al. (54) showed that a pressure probe in a large-scale fluidized bed can detect local pressure wave (due to, e.g., bubbles) up to a distance of about 0.5m from their origin.
4. *Filtering of the signal.* As with any measured signal, proper low-pass filtering should be applied at half the sample frequency or lower (satisfying the Nyquist criterion) to avoid signal distortion due to aliasing. In addition, it is recommendable to apply a high-pass filter to remove slow trends from the signal, especially for absolute pressure measurements. A typically cut-off frequency that can be used is 0.1 Hz. This prevents the signal from slowly moving out of the measurement range.
5. *Time-series length.* To be able to derive statistically sound results from the measurements, the data series should be sufficiently long. The proper length strongly depends on the type of analysis. For example, a time-series length up to 30 minutes is recommended for spectral and non-linear analysis (55,56).

Origin of pressure fluctuations

Although pressure signals are relatively easy to measure, their interpretation is not straightforward. In fact, there has been much debate about the origin of pressure fluctuations measured in fluidized beds (e.g., 57,58,59), with most of the attention aimed at bubbling beds. It appears that the measured pressure signal is a combination of (1.) local *bubble passages* and (2.) non-local *compression waves*; the latter resulting from a number of hydrodynamic phenomena.

1. Bubble passages. When a gas bubble rising upwards through the fluidized bed passes the measurement position, a pressure fluctuation is generated with a characteristic shape described by the Davidson (60) model; a more detailed description of this model was given by Davidson and Harrison (61). The model assumes an infinitely wide fluidized bed. However, for small diameter columns the effect of the moving bed mass should be included (62). In the lower part of a bubbling bed, bubble passage has a relatively small contribution to the pressure fluctuations. When moving in the upward direction, the contribution becomes larger (63). The reason is that the bubble diameter increases with increasing height, while the amplitude of the compression waves decreases with increasing height.

2. Compression waves. Compression waves can propagate both upwards and downwards through the bed. In a small diameter fluidized bed, the amplitude of a downward travelling compression wave stays constant; the amplitude of an upward travelling compression wave decreases linearly to zero at the bed surface (59). The fast-travelling compression waves can originate from a number of sources:

a. *Bubble generation.* To form a gas bubble at the distributor plate, the particles need to be accelerated upwards. Kage et al. (64) showed that the bubble generation frequency is one of the main frequencies in the power spectrum of plenum pressure fluctuations; in their experiments, bubbles were generated in groups.
b. *Bubble coalescence.* Fan et al. (57) were the first to ascribe pressure fluctuations to bubble coalescence. They showed that in the bottom section of a fluidized bed, pressure waves propagate downwards and upwards from within the bed.
c. *Bubble eruption.* The third source of compression waves is the eruption of bubbles at the surface of the bed. When the top of a bubble reaches the bed

surface, the actual bed height decreases at that position, leading to a decrease in the pressure below the erupting bubble (65).

d. *Gas flow fluctuations.* Fluctuations in gas flow are also a source for pressure fluctuations in a fluidized bed. This source becomes increasingly important when the pressure drop over the distributor plate is low, giving a high interaction between the gas supply system and the fluidized bed (66). A chain of bubbles can provide for a short-cut for the gas, leading to a temporary increase in gas flow. Van der Schaaf et al. (67) studied the phenomenon of gas velocity fluctuations for circulating fluidized beds, but this also applies to bubbling fluidized beds. Gas flow fluctuations are closely related to the generation, coalescence, and eruption of bubbles.

Bed mass oscillation cannot be seen apart from the sources of compression waves listed above. Bubble formation makes the bed mass rise, whereas bubble eruption makes it go down again. Moreover, increased gas flow through bubble chains will also be strongly connected to bed oscillation.

Deriving bubble sizes

Since a pressure fluctuation signal measured at a single position is a combination of bubble passage waves and compression waves, measurements at multiple positions are needed to derive the bubble characteristics. By measuring the differential pressure between two nearby points, the major part of the fast compression waves is removed from the signal. Sitnai (68) used four pairs of differential pressure probes to estimate bubble sizes and velocities. Clark et al. (69) showed that, in principle, one differential pressure transducer connected to two vertically spaced probes is sufficient to obtain these bubble characteristics. Ramayya et al. (70) used simulated data to show that it is also possible to obtain similar information from vertically spaced probes. Clark et al. (69) demonstrated their approach using data from a slugging fluidized bed. This is easier than freely bubbling fluidized bed data in which bubbles vary in size and are pierced by the probe at different positions, resulting in a chord distribution. Clark et al. (71) proposed a method to obtain a local bubble-size distribution from chord-length data derived from differential pressure measurements obtained in a freely bubbling bed. Santana and Macías-Machín (72) proposed an improved method that could cope with bubbles rising at an angle. Both methods are tested with synthetic data, but not with actual fluidized bed data. Moreover, they require prior knowledge of the shape of the bubbles. An alternative approach to obtain the bubble size distribution by statistical analysis of absolute pressure fluctuations measurement at one position is proposed by Bai et al. (73). They propose a relationship between the probability density function of the pressure fluctuations and the bubble size distribution. Application of this method to fluidized bed data shows the proper trends, but more work is needed to obtain a thorough validation.

Whereas deriving the bubble size distribution from pressure signals remains awkward, van der Schaaf (63) proposed a power spectral decomposition method to obtain the time-averaged bubble diameter at a given height using two absolute pressure fluctuation measurements. One probe is placed in the windbox, the other probe in the bed at the position were the average bubble diameter should be determined. The windbox measurement is taken since it contains just compression waves. If the pressure drop over the distributor is too high and hinders transmission of the compression waves from bed to windbox too much, a measurement position just above the distributor plate can be used instead. Using the windbox measurement, the power spectral density of the bed signal is decomposed into a part generated by global phenomena (the coherent part) and a part generated by local phenomena (the incoherent part). This is done using the coherence function, the counterpart of the cross-correlation in the frequency domain. The incoherent part of the power spectrum can be converted into an incoherent standard deviation, which is proportional to the average bubble diameter. This proportionality constant is independent of gas velocity and measuring height, but varies with bed diameter and bed material (63,74). This makes the method suitable to assess changes in bubble size due to, for example, electric fields and gas injection (75). However, the power spectral decomposition method cannot be used to directly obtain bubble sizes without calibration by a different measurement technique.

Other applications
In most cases, pressure fluctuation measurements are used to determine changes in the voidage distribution without the need to determine the voidage in a quantitative way. For example, pressure fluctuation measurements can be used for regime characterization (55), early detection of agglomeration (76), and potentially for control of a fluidized bed (77).

Acoustic measurements
The installation of pressure taps penetrating the vessel wall is sometimes constrained by severe process conditions or costs, especially in industrial units operated at high pressure. In those cases, passive acoustic measurements by a microphone attached at the outside of the wall might be an alternative (78). Since the signals obtained in this way are even more complicated than in-bed measured pressure signals, they are only used to obtain qualitative information about the state of fluidization (e.g., 79,80,81) To the authors' best knowledge, active acoustic measurements in which pressure waves are imposed on the system are hardly applied in fluidized beds.

CONCLUSIONS

Various techniques are available to determine the gas-solids distribution in fluidized beds. Direct visualization can be useful, but is limited to very dilute systems, pseudo 2-D beds, and the outer layer of dense, 3-D systems. Tomography is frequently used to obtain the voidage distribution in a horizontal cross-section of the bed. Electric capacitance tomography is fast, but its spatial resolution is limited and image reconstruction is troublesome. For nuclear (X-ray and gamma-ray) tomography, the image reconstruction is much easier and the spatial resolution better, but its temporal resolution is much lower. Currently, research for both techniques is aimed at reaching high spatial and temporal resolution. Optical probes and capacitance probes determine the voidage as a function of time in a small measurement volume. These probe techniques are reasonably well-developed; the current research effort spent at improving them seems limited, especially for capacitance probes. Time-averaged pressure measurements are commonly used to determine the average bed density and bed height. Obtaining quantitative voidage data from pressure fluctuations measurement remains a difficult task; in-bed pressure fluctuation and acoustic measurements are mostly used to determine changes in the voidage dynamics and distribution.

ACKNOWLEDGEMENTS

We would like to thank M.O. Coppens, J. Nijenhuis, R.W.S Bohlken, and M.A. Wormsbecker for useful suggestions during preparation of this manuscript.

REFERENCES

1. Grace, J.R., Baeyens, J., 'Instrumentation and experimental techniques', in D. Geldart (ed.), Gas fluidization technology, Wiley, Chichester, USA, 415-462, 1986.
2. Cheremisinoff, N.P., 'Review of experimental methods for studying the hydrodynamics of gas-solid fluidized beds', Ind. Eng. Chem. Process Des. Dev. 25, 329-351, 1986.
3. Yates, J.G., Simons, S.J.R., 'Experimental methods in fluidization research', Int. J. Multiphase Flow 20 Suppl., 297-330, 1994.
4. Louge, M., 'Experimental techniques', in: Grace, J.R., Avidan, A.A., Knowlton, T.M., Circulating Fluidization beds, Chapman & Hall, London, UK, 312-368, 1997.
5. Werther, J., 'Measurement techniques in fluidized beds', Powder Technol. 102, 15-36, 1999.
6. Chaouki, J., Larachi, F., Dudukovic, M.P. (Eds.), 'Non-invasive monitoring of multiphase flows', Elseviers, Amsterdam, the Netherlands, 1997.
7. Horio, M., Kuroki, H., 'Three-dimensional flow visualization of dilutely dispersed solids in bubbling and circulating fluidized beds', Chem. Eng. Sci., 49, 2413-2421, 1994.
8. Lackermeier, U., Rudnick, C., Werther, J., Bredebusch, A., Burkhardt, H., 'Visualization of flow structures inside a circulating fluidized bed by means of laser sheet and image processing', Powder Technol. 114, 71-83, 2001.
9. Lim K.S., Agarwal P.K., O'Neill B.K., 'Measurement and modelling of bubble parameters in a two-dimensional gas-fluidized bed using image analysis', Powder Technol. 60, 159-171, 1990.
10. Mudde, R.F., Schulte, H.B.M., van den Akker, H.E.A., 'Analysis of a bubbling 2-D gas-fluidized bed using image processing', Powder Technol. 81, 149-159, 1994.
11. Goldschmidt, M.J.V., Link, J.M., Mellema, S., Kuipers, J.A.M., 'Digital image analysis measurements of bed expansion and segregation dynamics in dense gas-fluidised beds', Powder Technol. 138, 135-159, 2003.
12. Simons, S. J. R., 'Imaging techniques for fluidized bed systems: A review', Chem. Eng. J. 56, 83-93, 1995.
13. Yates, J.G., Cheesman, D.J., Sergeev, Y.A., 'Experimental observations of voidage distribution around bubbles in a fluidized bed', Chem. Eng. Sci. 49, 1885-1895, 1994.
14. Kühn, F., 'Electrical capacitance tomography – development and application to fluidised beds', PhD thesis, Delft University of Technology, 1998.
15. Machida, M., Scarlett, B., 'Monitoring particle flows by displacement current sensing', in Proc. 1st World Congr. Industrial Process Tomography II, Buxton, U.K., 560–562, 1999.
16. Dyakowski, T., Jeanmeure, L.F.C., Jaworski, A.J., 'Applications of electrical tomography for gas-solids and liquid-solids flows - A review', Powder Technol. 112, 174-192, 2000.
17. Kühn, F., van Halderen, P.A., 'Design of an active-differentiator-based capacitance transducer for electrical capacitance tomography', Meas. Sci. & Techn. 8, 947-950, 1997.
18. Wang, M., Ma, Y., Holliday, N., Dai, Y., Williams, R.A., Lucas, G., 'A high-performance EIT system', IEEE J. Sensors, 5, 289-299, 2005.
19. Liu, S., Chen, Q., Wang, H.G., Jiang, F., Ismail, I., Yang, W.Q., 'Electrical capacitance tomography for gas-solids flow measurement for circulating fluidized beds', Flow Meas. Instrum. 16, 135-144, 2005.
20. Fan, L.-S., Warsito, W., Marashdeh, Q., Park, A.-H.A., Du, B., 'Electrical Capacitance Volume Tomography (ECVT) for Process Imaging', in: Dhodpkar, S., Klinzing, G., Hrenya, C., Proc. 5th World Congress on Particle Technology, Orlando, USA, paper 147a, 2006.

21. Chaplin, G., Pugsley, T., van der Lee, L., Kantzas, A., Winters, C., 'The dynamic calibration of an electrical capacitance tomography sensor applied to the fluidized bed drying of pharmaceutical granule', Meas. Sci. Technol. 16, 1281-1290, 2005
22. Wang, H., Liu, S., Jiang, F., Yang, W.Q., '3D presentation of images with capacitance tomography', in: Proc. of 3rd World Congress on Industrial Process Tomography, 2–5 September, Banff, Canada, 331–336, 2003.
23. Warsito, W., Marashdeh, Q., Fan, L.-S., 'Electrical Capacitance Volume Tomography (ECVT): Sensor Design and Image Reconstruction', in: De Jong, A., Takei, M., Williams, R.A., Zeidan, M., Proc. 4th World Congress on Industrial Process Tomography, Aizu, Japan, 82-87, 2005.
24. Kumar, S.B., Moselmian, D., Dudukovic, M.P., 'A gamma-ray tomographic scanner for imaging voidage distribution in two-phase systems', Flow Meas. Instrum., 6,1, 1995.
25. Mudde, R.F., Harteveld, W.K., van den Akker, H.E.A., van der Hagen, T.H.J.J., van Dam, H., 'Gamma radiation densitometry for studying the dynamics of fluidized beds', Chem. Eng. Sci. 54, 2047-2054,1999.
26. Bruneau, P.R.P., Mudde, R.F., van der Hagen, T.H.J.J., 'Fast computed tomographic imaging within turbulent fluidized beds', In: Kantzas, A. (Ed.),Proc. 3rd World Congress on Industrial Process Tomography, Banff, Canada, 589-594 2003.
27. Bruneau, P.R.P., Mudde, R.F., van der Hagen, T.H.J.J., 'High-speed flow imaging using gamma-ray computed tomography', In: de Jong, A., Takei, M., Williams, R.A., Zeidan, M. (Eds), Proc. 4th World Congress on industrial Process Tomography, Aizu, Japan, 440-445, 2005.
28. Mudde, R.F., Bruneau, P.R.P., van der Hagen, T.H.J.J., 'Time-resolved gamma-densitometry imaging within fluidized beds', Ind. Eng. Chem. Res. 44, 6181-6187, 2005.
29. Tortora, P.R., Ceccio, S.L., O'Hern, T.J., Trujillo, S.M., Torczynski, J.R., 'Quantitative measurement of solids distribution in gas-solid riser flows using electrical impedance tomography and gamma densitometry tomography', Int. J. Multiphase Flow, 32, 972-995, 2006.
30. Weimer, A.M., Gyuere, D.C., Clough, D.E., 'Application of a gamma-radiation density gauge for determining hydrodynamics properties of fluidized beds', Powder Techol., 44, 179-194, 1985.
31. Bhusarapu, S., Fongarland, P. Al-Dahhan, M.H., Dudukovic, M.P., 'Measurement of overall solids mass flux in a gas-solid circulating fluidized bed', Powder Tech., 148, 158-171, 2004.
32. O'Hern, T., Trujillo, S.M., Torczynski, J.R., Tortora, P.R., Ceccio, S.L., 'Radial and axial profiles of solids loading in a gas-solid circulating fluidized bed', AIChE Annual Meeting, Cincinnati, OH, USA, 2005, p.159d, 2005.
33. Shollenberger, K. A., Torczynski, J. R., Adkins, D. R., O'Hern, T. J., and Jackson, N. B., 'Gamma-densitometry-tomography of gas holdup spatial distribution in industrial-scale bubble columns', Chem. Eng. Sci. 52, 2037-2048, 1997.
34. Johnsson, H., Johnsson, F., 'Measurements of local solids volume-fraction in fluidized bed boilers', Powder Technol. 115, 13-26, 2001.
35. Rundqvist, R., Magnusson, A., van Wachem, B.G.M., Almstedt, A.E., 'Dual optical fibre measurements of the particle concentration in gas/solid flows', Exp. Fluids 35, 572-579, 2003.
36. Liu, J., Grace, J.R., Bi, X., 'Novel multifunctional optical-fiber probe: I. Development and validation', AIChE J. 49, 6, 1405-1420, 2003.
37. Werther, J., Hage, B., Rudnick, C., 'A comparison of laser Doppler and single-fibre reflection probes for the measurement of the velocity of solids in a gas-solid circulating fluidized bed', Chem. Eng. Process., 35, 381, 1996.
38. Nova, S.R., Krol, S., De Lasa, H.I., 'CREC fiber-optic probes for particle velocity and particle clustering: Design principles and calibration procedures', Ind. & Eng. Chem. Res. 43, 18, 5620-5631, 2004.
39. Mainland, M.E., Welty, J.R., 'Use of optical probes to characterize bubble behavior in gas-solid fluidized beds', AIChE J. 41, 223-228, 1995.

40. Groen, J.S., De Haseth, D.C., Mudde, R.F., van den Akker, H.E.A., 'Local bubble properties in 40 and 80cm diameter fluidized beds', AIChE Symp. Ser. 93 (no. 317), 147-151, 1997.
41. Clark, N.N., Turton, R., 'Chord length distribution related to bubble size distribution in multiphase flows', Int. J. Multiphase Flow, 14, 4, 413-424, 1988.
42. Werther, J., Molerus, O., 'The local structure of gas fluidized beds - I. A statistically based measuring system', Int. J. Multiphase Flow 1, 103-122, 1973.
43. Almstedt, A.E., Olsson, E., 'Measurements of bubble behavior in a pressurized fluidized bed burning coal, using capacitance probes', Proc. 7th Int. Conf. Fluidized Bed Combustion, Philadelphia, PA, USA, 1982. ASME, New York, Vol. 1, 89-98.
44. Acree Riley, C., Louge, M., 'Quantitative capacitive measurements of voidage in gas-solid flows', Particul. Sci. Technol. 7, 51-59, 1989.
45. Soong, C.H., Tuzla, K., Chen, J.C., 'Identification of particle clusters in circulating fluidized bed', in: Avidan, A.A. (Ed.), Proc. 4th Int. Conf. on Circulating Fluidized Beds, Somerset, USA, 1993, 615-620.
46. Louge, M., Lischer, D.J., Chang, H., 'Measurements of voidage near the wall of a circulating fluidized bed riser, Powder Technol. 62, 269-276, 1990.
47. Lints, M., Glicksman, L.R., 'The structure of particle clusters near the wall of a circulating fluidized bed', AIChE Symp. Ser. 89 (no. 296), 35-47, 1993.
48. Wiesendorf, V., Werther, J., 'Capacitance probes for solids volume concentration and velocity', Powder Technol. 110, 143-157, 2000.
49. van Ommen, J.R., Schouten, J.C., vander Stappen, M.L.M., van den Bleek, C.M., 'Response characteristics of probe-transducer systems for pressure measurements in gas-solid fluidized beds: how to prevent pitfalls in dynamic pressure measurements', Powder Technol., 106, 199-218, 1999. Erratum: Powder Technol., 113, 217, 2000.
50. Geldart, D., Xie, H.Y., 'The use of pressure probes in fluidized beds of group A powders', in: Potter, O.E., Nicklin, D.J. (Eds.), Fluidization VII, Engineering Foundation, New York, USA, 749–756, 1992.
51. van Ommen, J.R., de Korte, R.-J., van den Bleek, C.M., 'Rapid detection of defluidization using the standard deviation of pressure fluctuations', Chem. Eng. Process., 43, 1329-1335, 2004.
52. Nijenhuis, J., Korbee, R., Lensselink, J., Kiel, J.H.A., van Ommen, J.R., 'A method for agglomeration detection and control in full-scale biomass fired fluidized beds', Chem. Eng. Sci. 62, 644-654, 2007.
53. Croxford, A.J., Harrison, A.J.L., Gilbertson, M.A., 'The optimisation of pressure measurements for the control of bubbling fluidised beds', Int. J. Chem. Reactor Eng. 3, paper A39, 2005. http://www.bepress.com/ijcre/vol3/A39
54. van Ommen, J.R., van der Schaaf, J., Schouten, J.C., van Wachem, B.G.M., Coppens, M.-O., van den Bleek, C.M., 'Optimal placement of probes for dynamic pressure measurements in large-scale fluidized beds', Powder Technol. 139, 264-276, 2004.
55. Johnsson, F., Zijerveld, R.C., Schouten, J.C., van den Bleek, C.M., Leckner, B., 'Characterization of fluidization regimes by time-series analysis of pressure fluctuations', Int. J. Multiphase Flow 26, 663-715, 2000.
56. Brown, R.C., Brue, E., 'Resolving dynamical features of fluidized beds from pressure fluctuations', Powder Technol., 119, 68-80, 2001.
57. Fan, L.T., Ho, T.-C., Hiraoko, S., Walawender, W.P., 'Pressure fluctuations in a fluidized bed', AIChE J., 27, 388-396, 1981.
58. M'chirgui, A., Tadrist, H., Tadrist, L., 'Experimental investigation of the instabilities in a fluidized bed origin of the pressure fluctuations', Phys. Fluids 9, 500-509, 1997.
59. van der Schaaf, J., Schouten, J.C., van den Bleek, C.M., 'Origin, propagation and attenuation of pressure waves in gas-solid fluidized beds', Powder Technol. 95, 220-233, 1998.
60. Davidson, J.F., 'Symposium on fluidization - discussion', Trans. I. Chem. E. 39, 230-232, 1998.
61. Davidson, J.F., Harrison, D., 'Fluidized Particles', Cambridge Univ. Press, New York, USA, 1963.

62. van der Schaaf, J., 'Dynamics of gas-solids fluidized beds: analysis of pressure fluctuations', Ph.D. thesis, Delft University of Technology, The Netherlands, 2002.
63. van der Schaaf, J., Schouten, J.C., Johnson, F., van den Bleek, C.M., 'Non-intrusive determination of bubble and slug length scales in fluidized beds by decomposition of the power spectral density of pressure time series', Int. J. of Multiphase Flow 28, 865-880, 2002.
64. Kage, H., Iwasaki, N., Yamaguchi, H., Matsuno, Y., 'Frequency analysis of pressure fluctuation in fluidized bed plenum', J. Chem. Eng. Jpn 24, 76-81, 1991.
65. Baskakov, A.P., Tuponogov, V.G., Filippovsky, N.F., 'Study of pressure fluctuations in a bubbling fluidized bed', Powder Technol. 45, 113-117, 1986.
66. Sasic, S., Johnsson, F., Leckner, B., 'Interaction between a fluidized bed and its air-supply system: some observations', Ind. Eng. Chem. Res. 43, 5730-5737, 2004.
67. van der Schaaf, J., Schouten, J.C., Johnsson, F., van den Bleek, C.M., 'Bypassing of gas through bubble chains and jets in circulating fluidized beds', in: Wether, J. (Ed.), Proc. 6th Int. Conf. on Circulating Fluidized Beds, Wurzburg, Germany, 47-52, 1999.
68. Sitnai, O., 'Utilization of the pressure differential records from gas fluidized beds with internals for bubble parameters determination', Chem. Eng. Sci. 37, 1059-1066, 1982.
69. Clark, N.N., McKenzie, E.A., Gautam, M., 'Differential pressure measurements in a slugging fluidized bed', Powder Technol. 67, 187-199, 1991.
70. Ramayya, A.V., Venkateshan, S.P., Kolar, A.K., 'Bubble detection with horizontal pressure gradient measurements in gas- fluidised beds', Powder Technol. 97, 77-84, 1998.
71. Clark, N.N., Liu, W., Turton, R., 'Data interpretation techniques for inferring bubble size distribution from probe signals in fluidized systems', Powder Technol. 88, 179-188, 1996.
72. Santana, D., Macías-Machín, A., 'Local bubble-size distribution in fluidized beds', AIChE J. 46, 1340-1347, 2000.
73. Bai, B., Gheorghiu, S., van Ommen, J.R., Nijenhuis, J., Coppens, M.-O., 'Characterization of the void size distribution in fluidized beds using statistics of pressure fluctuations', Powder Technol., 160, 81-92, 2005.
74. Kleijn van Willigen, F., van Ommen, J.R., van Turnhout, J., van den Bleek, C.M., 'Bubble size reduction in a fluidized bed by electric fields', Int. J. of Chem. Reactor Eng. 1, paper A21, 2003. http://www.bepress.com/ijcre/vol1/A21
75. Kleijn van Willigen, F., Christensen, D., van Ommen, J.R., Coppens, M.-O., 'Imposing dynamic structures on fluidised beds', Cat. Today 105, 560-568, 2005.
76. van Ommen, J.R., Coppens, M.-O., van den Bleek, C.M., Schouten, J.C., 'Early warning of agglomeration in fluidized beds by attractor comparison', AIChE J., 46, 2183-2197, 2000.
77. Harrison, A.J.L., Lim, C.N., Gilbertson, M.A., 'Modelling and control of the dynamics of bubbling fluidized beds', Proc. IMechE Part E: J. Process Mechanical Engineering, 220, 43-53, 2006.
78. Finney, C.E.A., Daw, C.S., Halow, J.S., 'Measuring slugging bed dynamics with acoustic sensors', KONA: Powder and Particle, 16, 125-135, 1998.
79. Tsujimoto, H., Yokoyama, T., Huang, C.C., Sekiguchi, I., 'Monitoring particle fluidization in a fluidized bed granulator with an acoustic emission sensor', Powder Technol. 113, 88-96, 2000.
80. Halstensen, M., de Bakker, P., Esbensen, K.H., 'Acoustic chemometric monitoring of an industrial granulation production process - a PAT feasibility study', Chemome. Intell. Lab. Syst. 84, 88-97, 2006.
81. Villa Briongos, J., Aragon, J.M., Palancar, M.C., 'Fluidised bed dynamics diagnosis from measurements of low-frequency out-bed passive acoustic emissions', Powder Technol. 162, 145-156, 2006.